UC Irvine
UC Irvine Previously Published Works

Title

The confinement of dilute populations of beam ions in the national spherical torus experiment

Permalink

https://escholarship.org/uc/item/2zm4f0gh

Journal

Nuclear Fusion, 43(9)

ISSN

0029-5515

Authors

Heidbrink, WW
Miah, M
Darrow, D
et al.

Publication Date

2003-09-01

DOI

10.1088/0029-5515/43/9/312

Peer reviewed

The confinement of dilute populations of beam ions in the national spherical torus experiment

W.W. Heidbrink[1]**, M. Miah**[1]**, D. Darrow**[2]**, B. LeBlanc**[2]**,
S.S. Medley**[2]**, A.L. Roquemore**[2] **and F.E. Cecil**[3]

[1] University of California, Irvine, California, USA

[2] Princeton Plasma Physics Laboratory, Princeton NJ, USA

[3] Colorado School of Mines, Golden, Colorado, USA

Abstract

Short $\sim$3 ms pulses of 80 keV deuterium neutrals are injected at three different tangency radii into the national spherical torus experiment. The confinement is studied as a function of tangency radius, plasma current (between 0.4 and 1.0 MA), and toroidal field (between 2.5 and 5.0 kG). The jump in neutron emission during the pulse is used to infer prompt losses of beam ions. In the absence of MHD, the neutron data show the expected dependences on beam angle and plasma current; the average jump in the neutron signal is $88 \pm 39\%$ of the expected jump. The decay of the neutron and neutral particle signals following the blip are compared to the expected classical deceleration to detect losses on a 10 ms timescale. The temporal evolution of these signals are consistent with Coulomb scattering rates, implying an effective beam-ion confinement time $\gtrsim$100 ms. The confinement is insensitive to the toroidal field despite large values of $\rho \nabla B/B$ ($\lesssim$0.25), so any effects of non-conservation of the adiabatic invariant μ are smaller than the experimental error.

1. Introduction

Dilute populations of energetic ions exhibit excellent confinement properties in conventional tokamaks [1]. A spherical tokamak (ST) has a smaller major radius R relative to the minor radius a than a conventional tokamak; for example, in the national spherical torus experiment (NSTX), $a/R \simeq 0.7$. This difference has several implications of potential importance for fast-ion confinement. First, the magnitude of the poloidal field can be comparable to the toroidal field, altering the orbit topology [2, 3] and particle drifts [4]. Second, the relatively weak magnetic field B implies a large fast-ion gyroradius ρ, while the small value of the major radius implies rapid field variations ($B \propto 1/R$ in a torus). Because $\rho \nabla B/B$ is appreciable, the magnetic moment $\mu = W_\perp/B$, which is a robust adiabatic invariant in a conventional tokamak, need not be conserved in a ST [5–10]. In addition to these theoretical considerations, the confinement of fast ions in a ST is of considerable practical importance. Neutral beams are the primary heating system for thermal confinement studies in NSTX, so it is vital to understand their performance. Moreover, the normalized beam-ion gyroradius ρ/a in NSTX is comparable to the expected normalized gyroradius of alpha particles in a deuterium–tritium ST reactor, so measurements

of beam-ion confinement in NSTX address the viability of the ST as a fusion reactor.

The first study of fast-ion confinement in an ST was performed on the START ST [5]. The measured neutral particle spectra were consistent with predictions based on orbit calculations in the presence of Coulomb scattering alone.

Short neutral-beam pulses (beam 'blips') are a convenient technique [11] for the study of the confinement of dilute populations of beam ions. The technique has verified classical deceleration [11, 12] and weak diffusion [13, 14] of beam ions in conventional tokamaks, has measured anomalies associated with field ripple in conventional tokamaks [15–17] and has diagnosed poor confinement of perpendicular beam ions in the CHS helical device [18]. This paper reports the first application of the beam-blip technique to a ST. Although the scatter in the data is larger than expected, the absolute magnitude, time evolution and parametric dependences of the resulting neutron signals are consistent with classical beam-ion behaviour.

2. Experimental conditions and techniques for analysis

All the data in this paper were acquired during two consecutive days of operation in July 2001. Three neutral beam sources
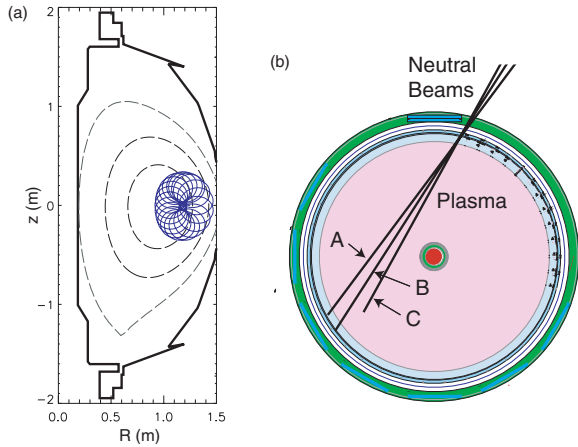
Figure 1. (*a*) Elevation of NSTX showing the vaccum vessel (——), the projection of an orbit of an 80 keV deuterium ion that is born near $R = 1.3$ m with $v_\parallel/v = 0.53$ (——), and some flux surfaces (dashed lines) for one of the experimental equilibria (discharge #105 753 at 220 ms). (*b*) Plan view of NSTX showing the angles of injection of the three neutral beam sources.
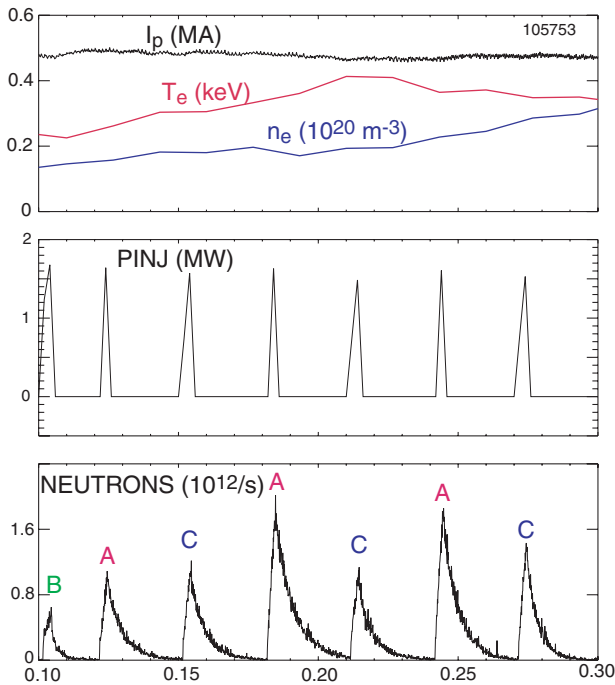

Figure 2. Plasma current, core electron temperature and density, beam power, and neutron rate for a typical discharge. The letters over the neutron trace indicate the beam source. (The 'core' T_e and n_e values are the average of the three most central Thomson scattering measurements.)

injected approximately 1.6 MW of ~80 keV deuterons into deuterium NSTX plasmas ($a \simeq 0.66$ m, $R \simeq 0.95$ m, elongation $\kappa \simeq 1.8$) at tangency radii of 0.69 m (Source A), 0.59 m (Source B), and 0.49 m (Source C). The gyroradius of a typical orbit is quite large, as illustrated in figure 1.

In a typical discharge (figure 2), several beam blips of ~3 ms duration are injected into a nominally steady-state portion of the discharge. The electron temperature and density are measured by a ten-point Thomson scattering diagnostic
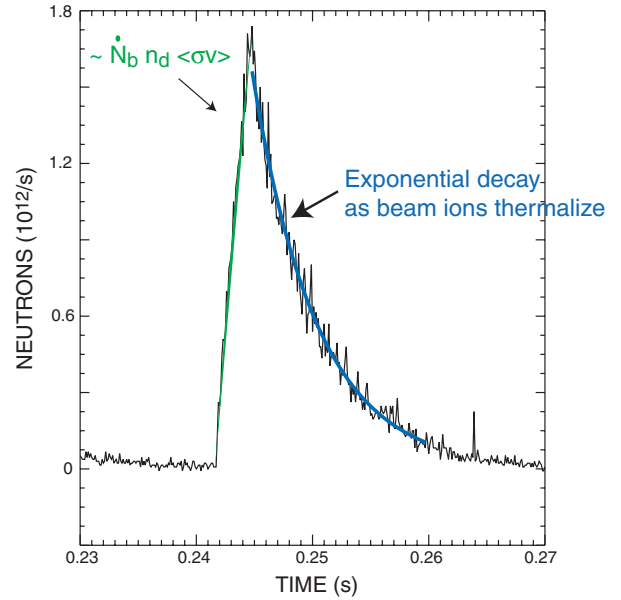

Figure 3. Detail of the neutron signal for the discharge of figure 2. The smooth lines are the fitted curves based on the model equations.

[19]. The relatively low central electron temperature of $T_e \lesssim 1$ keV implies that, classically, beam ions slow down primarily on thermal electrons. Accordingly, the classical pitch-angle scattering rate ν_{PAS} is an order of magnitude smaller than the energy deceleration rate ν_E. Under these conditions, in a conventional tokamak, pitch-angle scattering from a confined orbit to an unconfined orbit (across a loss boundary) happens rarely. The ion temperature and plasma rotation were not measured in these experiments but the classical confinement and neutron rate are insensitive to T_i and v_ϕ in this parameter regime. The effective charge of the plasma Z_{eff} is obtained from Thomson scattering measurements and a visible bremsstrahlung diagnostic [20]; $Z_{eff} \simeq 2.6$ is typical. The neutron rate is measured by a ZnS scintillator that was cross-calibrated to a 1.3 g ^{235}U detector, which was directly calibrated by a standard ^{252}Cf radioactive source [21].

At a typical beam blip (figure 3), the neutron emission I_n rises nearly linearly during the beam pulse, then decays approximately exponentially following the pulse. Under these conditions, the beam–plasma reaction rate is over an order of magnitude larger than the beam–beam or thermonuclear rates. The maximum possible rate of change of neutron emission is

$$\dot{I}_n \simeq \dot{N}_b n_d \langle \sigma v \rangle, \qquad (1)$$

where $\dot{N}_b$ is the rate at which full-energy beam ions are injected into the device, n_d is the deuterium density in the centre of the device, and $\langle \sigma v \rangle$ is the d–d reactivity. For these beam–plasma reactions with injection energy $E_{inj} \gg T_i$ (and negligible toroidal rotation), the reactivity is well approximated by the reactivity of an 80 keV deuteron that collides with cold target ions, $\langle \sigma v \rangle \simeq \sigma v = 3.39 \times 10^{-18}$ cm^3 s^{-1}. In a large, conventional tokamak with excellent confinement, nearly all the injected neutrals become centrally confined beam ions, so $\dot{N}_b \simeq f_{full} P_{inj}/E_{inj}$ where $f_{full} \simeq 0.66$ is the fraction of the total power carried by full-energy beam ions and P_{inj} is the injected power. For NSTX parameters, the maximum expected rate of

rise of the neutron emission is typically $\dot{I}_n = 279n_d$ (n_d is in cm^{-3} and $\dot{I}_n$ is in neutrons s^{-2}).

Following the blip, the neutron emission decays approximately exponentially. Because the reactivity decreases rapidly with energy, the expected neutron decay rate, $1/\tau_n$, is faster than the energy deceleration rate ν_E. A simple but accurate estimate of the expected decay time is given by a 'typical particle model' [22] using average values of T_e and n_e in the central third of the plasma:

$$\tau_n = (2.63\nu_E)^{-1}, \qquad (2)$$

where ν_E is the classical deceleration rate [23, 24] of 80 keV deuterons.

In an ideal beam blip experiment, the duration of the beam blip is short compared to the deceleration time, so an approximately monoenergetic population of beam ions is studied. In practice, τ_n can be comparable to the pulse duration t_{blip}. The resulting slight curvature of the rate of rise is evident in figure 3. To include this effect, the neutron signal is fit to the equation $\dot{I}_n = c - I_n/\tau_n$ during the beam blip and to $\dot{I}_n = -I_n/\tau_n$ after the pulse. The constant c reflects the prompt confinement of the injected beam ions and should equal the right-hand side of equation (1) if all the injected beam ions are confined in the plasma centre. The decay time τ_n should agree with the classical expectation (equation (2)) if delayed losses on the deceleration timescale are negligible. Empirically, the fit of the neutron signal to the temporal evolution predicted by this simple model is usually excellent (reduced $\chi^2 \ll 1$), as illustrated in figure 3.

Deviations from this model behaviour are sometimes observed, especially in the presence of violent MHD activity. In the example shown in figure 4, the plot of the rate of increase of the neutron signal is slightly concave (in contrast to the usual convex one) because of the bursts at 181 and 182 ms and the decaying signal abruptly terminates at the minor disruption at 191 ms, evidently indicating a total loss of beam-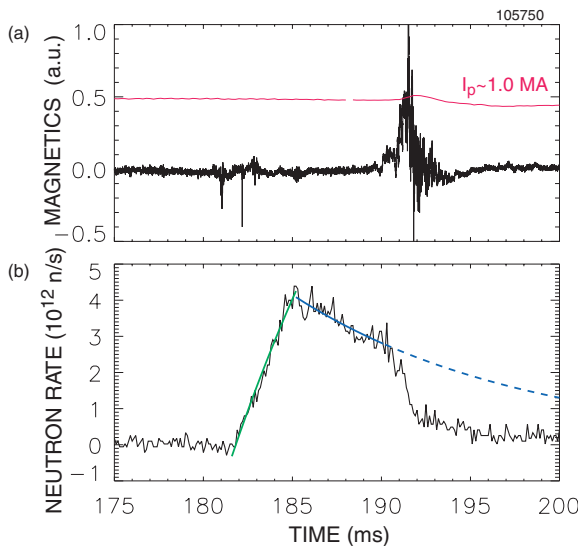ion confinement. (Minor disruptions were common during the 2001 experimental campaign but are now less prevalent due to improved vacuum conditions, reduced error fields, and increased operational experience [25].) Beam blips with concurrent low-frequency MHD activity are excluded from the data presented in the next section.

Beam ions in NSTX often destabilize modes with frequencies between 50 kHz and several megahertz. In these experiments, the beam population is intentionally kept small in order to study classical confinement. No evidence of any TAE [26] or CAE [27] activity is observed by magnetic diagnostics for any of the discharges reported here.

In addition to comparisons with simple test particle models, the data are compared to the predictions of the TRANSP code [28], which has been modified for NSTX to properly average plasma parameters over the relatively large beam-ion gyroradius [29]. The TRANSP code assumes conservation of the magnetic moment μ. The same algorithm used for the experimental data is used to fit the neutron signals predicted by TRANSP. This model is generally an excellent fit to the predicted time evolution.

3. Results

In a tokamak, the prompt losses of beam ions decrease with increasing plasma current because the poloidal gyroradius decreases. These losses are greater for perpendicular ions than for parallel ions. These expected trends are evident in figure 5, which shows the measured rate of rise of the neutron signal as a function of the plasma current. As expected, the jump in the neutron signal is larger for beam ions injected tangential to the field (Source A) than for beam ions injected at a more perpendicular angle (Source C). (This difference is also evident in the raw signal shown in figure 2). As expected, the signal strength increases with plasma current for all angles of injection.

The scatter of the data in figure 5 is large. Known sources of error include the following.

- Uncertainties associated with fitting the neutron data to the model rise and decay equations are ~10%.
- The rise depends on the deuterium density n_d, which itself depends on both the electron density n_e and Z_{eff}. The random error in the Thomson scattering measurements

Figure 4. (a) $\dot{B}_\theta$ signal from a probe mounted near the outer wall. The plasma current is also shown. (b) Neutron signal: the smooth lines are the fitted curves based on the model equations.
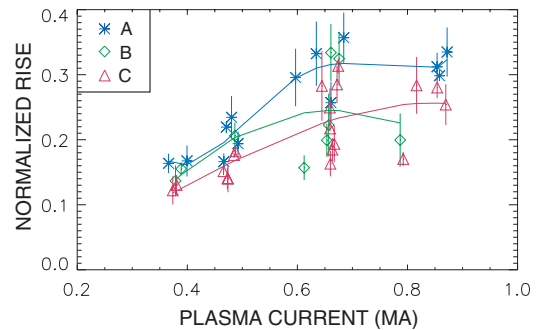

Figure 5. Measured rate of increase of the neutron signal divided by the ideal rate (equation (1)) vs I_p for all beam blips with undetectable MHD activity and $B_T > 0.3$ T. The symbols denote the angle of beam injection. The error bars are derived from estimates of the uncertainties in the model fit and in the deuterium density. The curves are from polynomial least-square fits to the data.
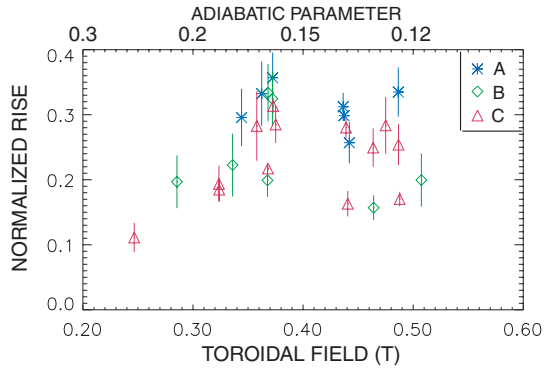
Figure 6. Measured rate of increase of the neutron signal divided by the ideal rate (equation (1)) vs B_T for all beam blips with undetectable MHD activity and $I_p > 0.5$ MA. The symbols denote the angle of beam injection. The error bars are derived from estimates of the uncertainties in the model fit and in the deuterium density. The upper axis is the approximate value of $\rho \nabla B / B$.

Figure 7. Measured neutron decay time τ_n divided by the classically expected decay time (equation (2)) vs B_T for all beam blips with undetectable MHD activity. The symbols denote the angle of beam injection. The error bars are derived from estimates of the uncertainties in the model fit and in the classical deceleration rate. The upper axis is the approximate value of $\rho \nabla B / B$.

of electron density is typically 5%; the systematic error is estimated as ~5%. In addition, measurements are only acquired every 17 ms. In the analysis, the average of the density measurements before and after the blip is employed but rapid changes in density introduce additional errors.

- The Z_{eff} measurement is an average value. The uncertainty is difficult to quantify but could be substantial. It is also assumed that carbon is the dominant impurity, so $n_d/n_e = (Z_{eff} - 1)/(6 - 1)$, but this may not always be the case.
- The neutral beams were not calibrated to measure the time evolution of the beam power throughout the beam blip at the time of this experiment. Generally, the beam voltage and power are only available for a single time point during the blip. Any power fluctuations or error in this single measurement contributes to the overall error.
- The relative error in the neutron measurement is small and is included in the fitting uncertainties given above. On the other hand, the absolute error is estimated to be 25%.

For currents above 0.5 MA and fields above 0.25 T, the normalized rise in neutron rate is 0.42 ± 0.04 for Source A, 0.32 ± 0.10 for Source B, and 0.32 ± 0.06 for Source C. The absolute magnitude of the normalized rise is a factor of three smaller than the ideal value of unity but, as discussed below, this discrepancy is principally caused by the deficiencies of the typical particle model.

To investigate any effects associated with the large beam-ion gyroradius, the toroidal field is varied between 0.25 and 0.50 T. Any systematic variation in prompt losses is obscured by the relatively large scatter in the data (figure 6). Losses due to non-conservation of μ are more likely to appear as an effect on the decay rate but no systematic variation with toroidal field is observed (figure 7). There is also no difference in decay rates for different angles of injection. The ratio of τ_n to the prediction of the typical particle model (equation (2)) is 1.16 ± 0.25 for Source A, 1.06 ± 0.17 for Source B, and 1.05 ± 0.35 for Source C. Theoretically, the decay rate is not expected to depend significantly on the injection angle in a regime where Coulomb drag on electrons predominates, since pitch-angle scattering onto loss orbits is negligible for nearly
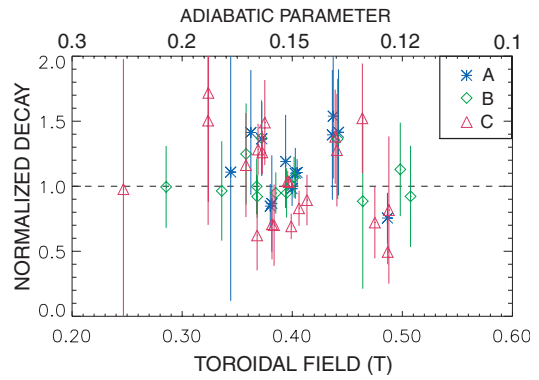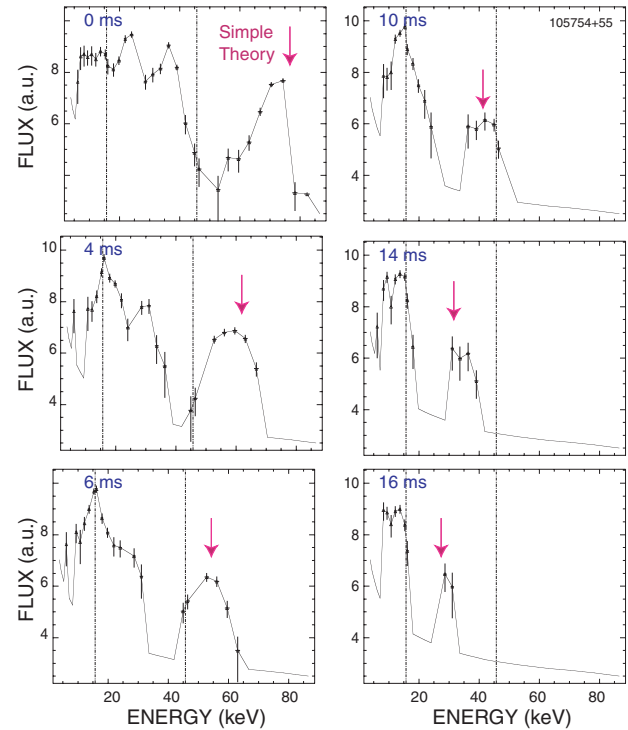

Figure 8. Neutral flux vs energy at various times after the end of a beam blip. The data are the sum of two nominally identical blips. The arrows indicate the classically predicted peak of the distribution using core values of T_e and n_e. Energy bins with zero counts are represented as one count plotted without an error bar. Source A, $I_p = 0.48$ MA, $B_T = 0.39$ T, $n_e \simeq 1.5 \times 10^{13}$ cm^{-3}, $T_e \simeq 0.3$ keV.

all initially confined orbits. In contrast to the rise in neutron emission, the decay time is in good agreement with the simple theoretical prediction, indicating that well-confined, centrally born beam ions slow down classically.

The good agreement of the measured decay time with classical Coulomb scattering theory is corroborated by neutral particle measurements (figure 8). For these measurements, the analyser [30] is oriented to measure the same tangency radius as injected by Source A. The spectra are produced by
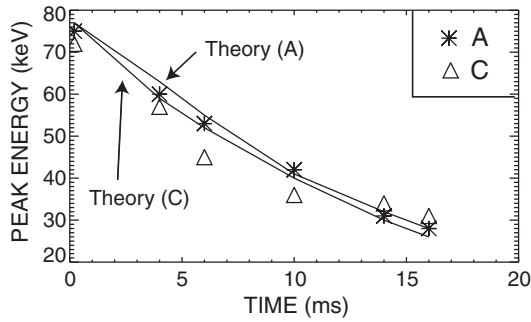
Figure 9. Energy of the full energy beam ions with the largest flux vs time for the Source A beam blip at 124 ms (∗) and the Source C beam blip at 154 ms (△) in discharges #105 754 and #105 755. (Raw neutral particle data for Source A appears in figure 8.) Also shown is the classically predicted peak of the distribution using core values of T_e and n_e (——).
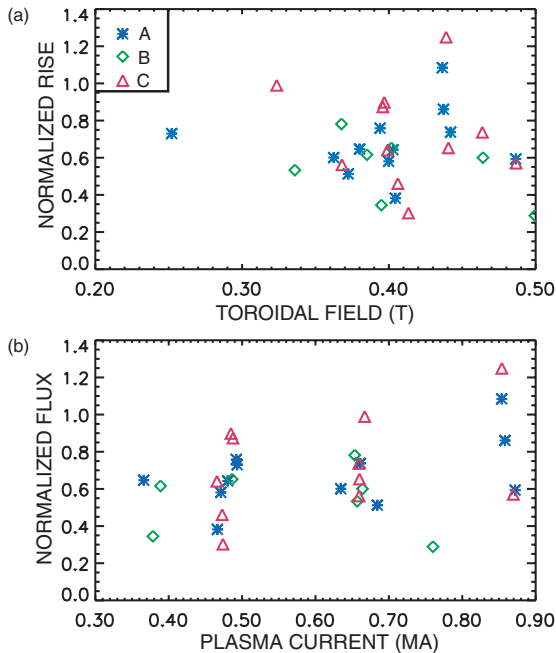

Figure 11. Measured neutron decay time τ_n divided by the TRANSP prediction vs the TRANSP prediction for all beam blips with undetectable MHD activity. The symbols denote the angle of beam injection. The error bars are derived from estimates of the uncertainties in the model fit and in the classical deceleration rate. The dashed line is the best linear fit to the data with decay times $\tau_n > t_{blip}$.

Figure 10. Measured rate of increase of the neutron signal divided by the TRANSP prediction vs (*a*) B_T and (*b*) I_p for all beam blips with undetectable MHD activity. The symbols denote the angle of beam injection.

'passive' charge-exchange between the ambient neutral density profile and the beam ions, so the spatial dependence of the signal is complicated. If one assumes that the signal originates predominantly in the plasma core, the energy should decrease as $E = E_0 \exp(-\nu_E t)$, where ν_E is evaluated using central values of T_e and n_e. As shown in figures 8 and 9, this simple estimate is in good agreement with the measurement. The deceleration rate is similar for Sources A and C, as expected.

The neutron data are also compared to the predictions of the TRANSP code, which includes beam deposition calculations, averaging of the Coulomb drag and fusion rates over particle orbits, and charge-exchange losses (figure 10). With the inclusion of these effects, the predicted jump in the neutron emission rate is smaller than that predicted by the typical particle model, yielding acceptable agreement with the
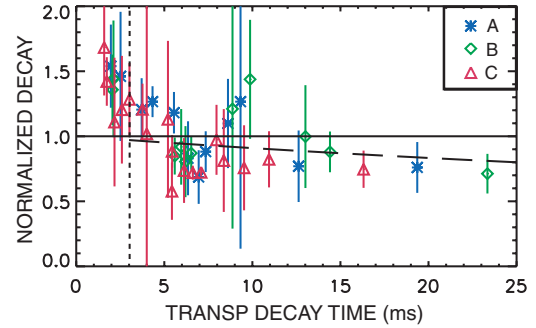
experiment. TRANSP predicts that ∼90% of the injected beam power is deposited in the plasma for the discharges with $I_p \simeq 1$ MA but only ∼50% is deposited for $I_p \simeq 0.4$ MA. Any systematic variation in prompt confinement with toroidal field is obscured by the relatively large scatter of the results. The ratio does not vary systematically with tangency radius or plasma current, indicating that the principal variations associated with the beam-ion drift orbits are properly modelled by TRANSP. The average ratio is $88 \pm 39\%$.

The measured decay time is in excellent agreement with the TRANSP predictions (figure 11). (For decay times that are short compared to the duration of the blip, the agreement is poorer but the measurements are less reliable.) According to TRANSP, half of the reactions occur in the central quarter of the plasma and 90% occur within $r/a < 0.5$, so the prediction of the typical particle model is valid for the decay time. The normalized decay time does decrease slightly with increasing decay time. This could indicate some deviation from classical behaviour on the timescale of ∼20 ms. To quantify this effect, assume a typical particle has a confinement time of τ_c. Rather than remaining at a constant value of unity, the normalized decay time is now expected to decrease as $[1+1/(2.63\nu_E\tau_c)]^{-1}$. The best fit to the data in figure 11 implies an effective confinement time of ∼100 ms.

Direct beam-ion losses to the midplane of the outer vacuum vessel wall are measured by a set of foils that act as Faraday cups [31]. In some cases, positive current is measured during the beam blip; no detectable current is observed after any of the beam blips. When current is detected, it is largest on the foil that is closest to the plasma ($R = 1.61$ m) and is smaller on the foils at $R = 1.63$ and 1.66 m. To analyse the data, the signals are integrated over the beam pulse to obtain the total collected charge. The correlation of the detected charge with other plasma parameters and with the neutron measurements is very weak; the strongest dependences are shown in figure 12. Evidently, lost beam ions do not reliably intersect the vessel wall at the poloidal location of the Faraday cups.

4. Conclusions

For all three injection angles, the prompt confinement is degraded for currents below 0.5 MA, as expected. The effect
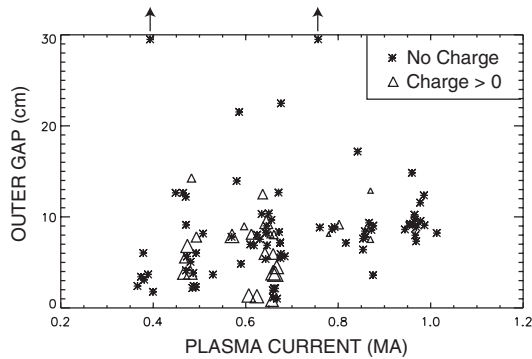
Figure 12. Parameter space for beam-ion loss detector data. The abscissa is I_p and the ordinate is the gap between the last-closed flux surface and the vacuum vessel. Usually, no charge is detected during a beam blip ($*$). The triangles indicate blips where charge is detected, with the symbol size proportional to $\log_{10}$ of the detected charge. The arrows indicate that the outer gap exceeds 30 cm.

is strongest for the most perpendicular injection angle, also as expected.

The magnitude of the jump in neutron emission is comparable to the expected value for all injection angles and values of poloidal and toroidal fields. On the other hand, the scatter in the neutron jump data is larger than that expected based on known uncertainties. A possible reason for this scatter is that the deuterium density may not be accurately inferred from a single visible bremsstrahlung chord. Alternatively, variable prompt losses on a timescale much shorter than 1 ms may be occurring.

The temporal evolution of the neutron signal is in excellent agreement with the expectations of classical theory. Any delayed losses of initially confined beam ions are small ($\lesssim 15\%$) on a 20 ms timescale. The good agreement between the measured decay time and Coulomb scattering theory confirms the accuracy of the Thomson scattering measurements of central T_e and n_e (to within $\sim 15\%$).

Many NSTX plasmas have higher values of ion temperature than expected from classical energy transfer rates and neoclassical ion confinement [32]. The good agreement between the measured decay rates and classical Coulomb scattering theory suggests that the initially confined beam ions transfer their energy to electrons rather than to thermal ions, as expected. If any anomalous energy transfer to thermal ions occurs, it must occur on a sub-millisecond timescale.

Statistically significant variations in either prompt or delayed confinement with $\rho \nabla B / B$ are absent in these data (for values between 0.12 and 0.25). Recent theoretical studies [5–9] predict reductions that are smaller than the experimental uncertainty so, although this result is consistent with theory, it does not constitute a rigorous test of the predictions.

Although minor disruptions do degrade the beam-ion confinement, it seems unlikely that low-frequency MHD is responsible for the large scatter in the data. The level of MHD activity in the analysed data is at a much lower level than that which degrades beam-ion confinement in a conventional tokamak. Moreover, inclusion of beam blips taken during

stronger (but still low) MHD activity does not significantly alter the results presented in section 3.

Future work should focus on understanding the large variability in the signal levels. Similar studies for higher beta plasmas are also desirable.

Acknowledgments

References

[1] Heidbrink, W.W. and Sadler G.J. 1994 *Nucl. Fusion* **34** 535
[2] Mikkelsen D.R. *et al* 1997 *Phys. Plasmas* **4** 3667
[3] Redi M.H., Darrow D.S., Egedal J., Kaye S.M. and White R.B. 2002 Calculations of neutral beam ion confinement for the national spherical torus experiment 2002, EPS *Princeton Plasma Physics Laboratory Report* PPPL-3714
[4] Kolesnichenko Y.I., Marchenko V.S. and White R.B. 2001 *Phys. Plasmas* **8** 3143
[5] Akers R.J. *et al* 2002 *Nucl. Fusion* **42** 122
[6] Carlsson J. 2001 *Phys. Plasmas* **8** 4725
[7] Kolesnichenko Y.I., White R.B. and Yakovenko Y.V. 2002 *Phys. Plasmas* **9** 2639
[8] Yakovenko Y.V., Kolesnichenko Y.I. and White R.B. 2002 Lagrangian description of nonadiabatic particle motion in spherical tori *Technical Report* PPPL-3712 Princeton Plasma Physics Laboratory 2002
[9] Egedal J., Redi M.H., Darrow D.S. and Kaye S.M. 2003 *Phys. Plasmas* **10** 2372
[10] Yavorksij V.A. *et al* 2002 *Nucl. Fusion* **42** 1210
[11] Heidbrink W.W., Kim J. and Groebner R.J. 1988 *Nucl. Fusion* **28** 1897
[12] Heidbrink W.W. 1990 *Phys. Fluids* B **2** 4
[13] Heidbrink W.W. *et al* 1991 *Phys. Fluids* B **3** 3167
[14] Ruskov E., Heidbrink W.W. and Budny R.V. 1995 *Nucl. Fusion* **35** 1099
[15] Tobita K., Tani K., Nishitani T., Nagashima K. and Kusama Y. 1994 *Nucl. Fusion* **34** 1097
[16] Isobe M., Tobita K., Nishitani T., Kusama Y. and Sasao M. 1997 *Nucl. Fusion* **37** 437
[17] Ruskov E. *et al* 1999 *Phys. Rev. Lett.* **82** 924
[18] Isobe M. *et al* 2001 *Nucl. Fusion* **41** 1273
[19] Leblanc B.P. *et al* 2003 *Rev. Sci. Instrum.* **74** 1659
[20] Ramsey A.T. and Turner S.L. 1987 *Rev. Sci. Instrum.* **58**
[21] Johnson L.C. *et al* 1995 *Rev. Sci. Instrum.* **66** 894
[22] Strachan J.D. *et al* 1981 *Nucl. Fusion* **21** 67
[23] Trubnikov B.A. 1965 *Review of Plasma Physics* vol 1 (New York: Consultants Bureau)
[24] Book D.L. 1990 *NRL Plasma Formulary* (Washington, DC: Naval Research Laboratory)
[25] Menard J.E. *et al* 2003 IAEA 2002 paper
[26] Wong K.-L. 1999 *Plasma Phys. Control. Fusion* **41** R1
[27] Fredrickson E.D. *et al* 2001 *Phys. Rev. Lett.* **87** 145001
[28] Budny R.V. 1994 *Nucl. Fusion* **34** 1247
[29] Pankin A., Mccune D., Andre R., Bateman G. and Kritz A. 2003 The tokamak Monte Carlo fast ion module NUBEAM in the national transport code collaboration library *Comput. Phys. Commun.* submitted
[30] Medley S.S. and Roquemore A.L. 1998 *Rev. Sci. Instrum.* **69** 2651
[31] Darrow D.S. *et al* 2001 *Rev. Sci. Instrum.* **72** 784
[32] Leblanc B.P. *et al* 2002 *IAEA Lyon* paper EX/C5-2